

Quantum pseudo-integrable Hamiltonian impact systems.

Omer Yaniv and Vered Rom-Kedar

*Department of Computer Science and Applied Mathematics,
Weizmann Institute of Science, Rehovot 7610001, Israel*

(Dated: October 7, 2022)

Quantization of a toy model of a pseudointegrable Hamiltonian impact system is introduced, including EBK quantization conditions, a verification of Weyl's law, the study of their wavefunctions and a study of their energy levels properties. It is demonstrated that the energy levels statistics are similar to those of pseudointegrable billiards. Yet, here, the density of wavefunctions which concentrate on projections of classical level sets to the configuration space does not disappear at large energies, suggesting that there is no equidistribution in the configuration space in the large energy limit; this is shown analytically for some limit symmetric cases and is demonstrated numerically for some nonsymmetric cases.

Quantum chaos studies how classical dynamics (integrable and non-integrable) are reflected in the properties (e.g. eigenvalues and eigenfunctions) of the correspondent quantum system. It is accepted that in integrable systems, the distribution of the level spacing is provided by the Poisson distribution e^{-s} [1], while that in chaotic systems (hereafter, meaning mixing system on energy surfaces, studied by simulating chaotic billiards) they distribute as eigenvalues of random matrix ensembles (GOE) [2]. When a system has a mixed phase space, which is the common behavior of smooth Hamiltonian systems, it is found that a Berry-Robnik distribution, a convex hall of the Poisson and the GOE distributions, describes the level spacing [3, 4]. This distribution reflects the existence of eigenfunctions supported on the islands of stability and of eigenfunctions supported on the chaotic components of the classical phase-space [5].

Pseudointegrable dynamics, correspond to systems with intermediate complexity: the phase space trajectories are not ergodic on the full energy surface, yet, they are not always periodic or quasi-periodic. Such systems arise in the study of plane polygonal rational billiards (polygonal tables with all corners being rational fractions of π), where trajectories move on invariant two-dimensional surfaces of genus $g > 1$ [6, 7]. The level spacing in such quantum systems appears to have intermediate statistics: the nearest-neighbor distribution displays repulsion at small distances and an exponential decay at large distances [8].

Another important characteristic of quantum systems is the asymptotic distribution of their wavefunctions. For systems with classical ergodic dynamics, in the semiclassical limit, the eigenfunctions which are equidistributed form a density 1 sequence [9]. In particular, such wavefunctions are equidistributed in both configuration space and momenta space. The other wavefunctions, which are not equidistributed, have scars - they concentrate along invariant phase space sets or on singular sets of the classical dynamics [10, 11]. For chaotic billiards, the most visible scars are associated with low period unstable periodic orbits and orbits at corners of the billiard table [10, 12].

Since plane rational polygonal billiards are ergodic

only in the configuration space (and not in the momenta space), equidistribution of the wavefunctions can be expected only in their configuration representation. Following [9], it was established that also here, in the semiclassical limit, scars in configuration space can only appear for a vanishing density of eigenfunctions [13]. Yet, it was observed, for finite energies, that some of the exceptional wavefunctions here have superscars; these concentrate on invariant sets associated with families of classical periodic orbits [14]. Such structures were observed experimentally [15, 16].

In this letter we investigate eigenvalues statistics and eigenfunctions properties of a class of systems that belongs to the recently discovered family of classical pseudointegrable Hamiltonian systems with impacts. Such systems combine motion under a smooth potential field with continuous symmetries and reflections from a corresponding family of billiards that keeps the continuous symmetries only locally and not globally. For example, trajectories of a separable Hamiltonian

$$H = H_1 + H_2, \quad H_i(q_i, p_i) = \frac{p_i^2}{2m} + V_i(q_i), \quad i = 1, 2 \quad (1)$$

in a right-angled polygonal billiard with at least one concave corner are pseudointegrable [17, 18].

Here, we study the quantum step oscillators: we take V_i to be confining potentials which are even smooth functions with a single minimum at the origin and are monotone elsewhere, and take the right angled polygon to be $\mathbb{R}^2 \setminus S$, where

$$S_{q^{wall}} = \{(q_1, q_2) \mid q_1 < q_1^{wall} \leq 0 \text{ and } q_2 < q_2^{wall} \leq 0\}. \quad (2)$$

The trajectories are confined by the potential and reflect from the step $S_{q^{wall}}$ [17], see Figure 1a. Since the step boundaries are parallel to the axes, the vertical and horizontal momenta are conserved at reflections, so the motion occurs along the level sets $H_i(q_i, p_i) = E_i$, $i = 1, 2$. Passing to the action angle coordinates of the smooth separable system, provided $E_i > V_i(q_i^{wall})$, $i = 1, 2$, the motion on each level set is conjugated to the directed motion on the flat cross-shaped surface, see Figure 1b. The direction of motion on this surface is given by

$\omega_2(E_2)/\omega_1(E_1)$ and the cross shaped concave corners are at $\{\pm\theta_1^{wall}(E_1), \pm\theta_2^{wall}(E_2)\}$, where $\omega_i(E_i)$ denotes the frequency of the smooth periodic motion under H_i and $\theta_i^{wall}(E_i)$ denotes the angle of an impacting trajectory (with the convention that $\theta_i = 0$ at the maximum of q_i). So, the direction of motion and the surface dimensions depend continuously on (E_1, E_2) . For the case of harmonic oscillators, i.e. when $V_i(q_i) = \frac{1}{2}\omega_i q_i^2$, the frequencies are fixed at ω_i and the values of $\theta_i^{wall}(E_i)$ can be explicitly computed. Equivalently, by folding the surface, the motion on such level sets is conjugated to the directed billiard motion on an L-shaped billiard, see Figure (1)c. Thus, this system is pseudointegrable [17]. In general, the dynamics on such surfaces has non-trivial ergodic properties. It was proven that if $q_i^{wall} < 0$ for $i = 1, 2$, the motion is typically uniquely ergodic, and, for the case of resonant harmonic oscillators, there are level sets with co-existing periodic ribbons and dense orbits on some parts of the cross-shaped surface [18].

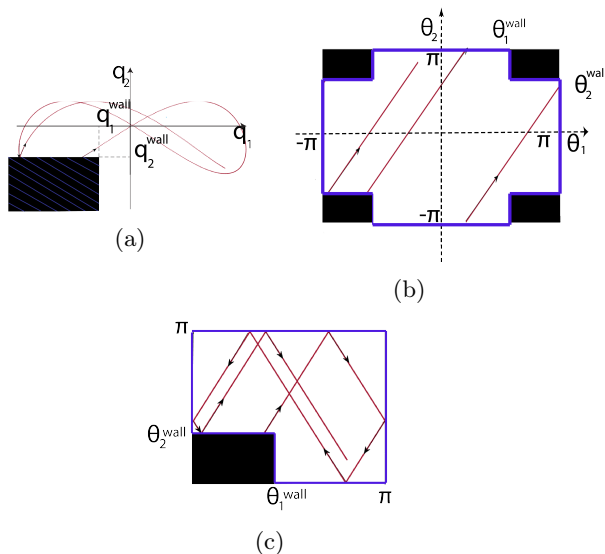


FIG. 1: A trajectory of a separable Hamiltonian reflecting from a step. (a) Projection to the configuration space. (b) The corresponding directed motion on the cross-shaped surface in the angles space. (c) Folding the surface to the lower left quadrant leads to the corresponding billiard motion on an L-shaped billiard. Here, Eq. (1) are integrated with elastic reflections from the step of Eq. (2), with $V_i(q_i) = \frac{1}{2}\omega_i q_i^2$, $\omega_1 = 1$, $\omega_2 = \sqrt{2}$, $q_1^{wall} = q_2^{wall} = -1$, $E_1 = 5.625$, $E_2 = 5.50$.

As we are interested in quantization, and, in particular, in studying the role of superscars in the system, we look first for families of periodic orbits. Given a family of periodic orbits on a given level set $(E_1, E_2 = E - E_1)$, with $\mu = (\mu_1, \mu_2)$ turning points (μ_1 in the horizontal direction and μ_2 in the vertical one), and $b = (b_1, b_2)$ impacts (b_1 with the right side of the step and b_2 with the upper part of the step), and an action $I(E; \mu, b)$, we

can quantize it by using the EBK quantization conditions [19, 20]:

$$I(E; \mu, b) = \hbar(n + \frac{\mu_1 + \mu_2}{4} + \frac{b_1 + b_2}{2}). \quad (3)$$

Moreover, denoting by $I_i(E_i)$ the action of the smooth H_i system and by $I_i^{wall}(E_i) = \int_{q_i \geq q_i^{wall}} p_i(q_i; E_i) dq_i = I_i \frac{2\theta_i^{wall}}{2\pi}$ the action of the impact H_i system, we obtain:

$$I(E_1, E_2; \mu, b) = \sum_{i=1}^2 b_i I_i^{wall} + (\frac{\mu_i - b_i}{2}) I_i, \quad (4)$$

namely, given $\mu, b, I_i(E_i)$ and $\theta_i^{wall}(E_i)$, we expect that the EBK quantization rule will predict the energy levels. Yet, in general, it is non-trivial to find μ and b (see e.g. section 7 in [18]) nor to invert $I(E_1, E_2; \mu, b)$ on the given family of periodic orbits.

We consider first some simple limit cases in which periodic motion can be easily identified. When the step is at the origin ($S_0 = S_{q_1^{wall}=q_2^{wall}=0}$), the corner angles are fixed at $\theta_i^{wall}(E_i)|_{q_1^{wall}=q_2^{wall}=0} = \frac{\pi}{2}$, so the dimensions of the cross-shaped surface are independent of the energy. When the potentials are harmonic, the direction of motion, ω_2/ω_1 is independent of the energy as well and $I_i = E_i/\omega_i$. Thus, by choosing resonant harmonic potentials and a step at the origin, we conclude that for all partial energies the motion is periodic and of the same type and that $I_i^{wall} = I_i/2$. In particular, setting: $\omega_1 = 1, \omega_2 = \frac{n}{m}$ (with $\gcd(n, m) = 1$), it can be shown that there are exactly 2 options for dynamics; When m is odd there is a single family of periodic orbits, whereas an even m leads to 2 distinct families of periodic orbits. In this latter case, one of the families has half of the action of the other one. Taking the simplest case of $n = 1$, we can compute the number of impacts and turning points for each of these families, and then, using Eqs. (3) and (4) provide a prediction for the eigenvalues, E_k . For odd m , we obtain that the periodic trajectory has $3(m+1)$ turning points ($\mu_1 = 3m, \mu_2 = 3$) and $m+1$ impacts ($b_1 = m, b_2 = 1$), hence

$$E_k = \frac{k}{1.5m} + \frac{5(1+m)}{6m}. \quad (5)$$

For even m we obtain that the first family of periodic orbits has $2(m+1)$ turning points ($\mu_1 = 2m, \mu_2 = 2$) and m ($b_1 = m, b_2 = 0$) impacts, whereas the second one has $m+1$ ($\mu_1 = m, \mu_2 = 1$) turning points and 1 impact ($b_1 = 0, b_2 = 1$), hence

$$E_{k_1}^I = \frac{k_1}{m} + \frac{4m+2}{4m} \quad (6)$$

$$E_{k_2}^{II} = \frac{2k_2}{m} + \frac{m+3}{2m}, \quad (7)$$

In figure 2, we validate the above results. Notice that for even m there are infinite number of energy levels at which $E_{k_1}^I = E_{k_2}^{II}$ (marked with green lines), and in particular,

for $m = 2$, $E_{k_1}^I = E_{2k_1}^{II}$ (as shown in Fig. 2). Since the system here is symmetric, all these energy levels are degenerate, and, as shown in 2b, the common energy levels for the two families have higher degeneracy.

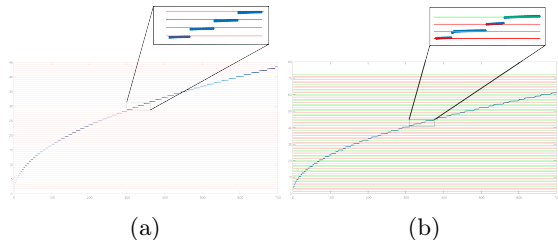


FIG. 2: Energy levels for resonant harmonic oscillator with a step at the origin: numerical and expected (EBK) values. (a) Odd m ($\omega_1 = 1$, $\omega_2 = 1$): the expected values for the single family of the periodic orbits of Eq. 5 denoted by horizontal red lines agree with the numerical values (blue dots). (b) Even m $\omega_1 = 1$, $\omega_2 = 2$: The expected values (family I:red and green horizontal lines, Family II: only green horizontal lines) agree with the numerical values, and the common values have larger degeneracy.

Next we use Weyl's law to validate our computations of correspondence between the classical families of periodic orbits and the energy levels. Recall that for the two dimensional case, Weyl's law is:

$$N[E_j : E_j \leq b] = \frac{1}{\hbar^2} \text{Vol}(H \leq b) + o(1) \text{ as } \hbar \rightarrow 0 \quad (8)$$

and notice that the phase space volume for the step-oscillator is:

$$\text{Vol}(\mathcal{E}) = \int_0^{I_2(\mathcal{E})} dI_2 \int_0^{I_1(\mathcal{E}-E(I_2))} -4\theta_1^{\text{wall}}(I_1)\theta_2^{\text{wall}}(I_2) + 4\pi(\theta_1^{\text{wall}}(I_1) + \theta_2^{\text{wall}}(I_2))dI_1. \quad (9)$$

For the case of a step at the origin and harmonic oscillators, we obtain

$$\text{Vol}(\mathcal{E})|_{S_0, \text{Harmonic oscillators}} = \frac{3\pi^2}{2\omega_1\omega_2} \mathcal{E}^2. \quad (10)$$

Fig. 3 shows this expected correspondence. For the even m case the contribution of the larger degeneracy associated with the energy levels which are common to the 2 different families is evident.

Next, we examine non-resonant oscillators (and not necessarily harmonic) while keeping the step at the origin. Classically, the motion is ergodic within the level set for almost all partial energies. Hence, we expect wavefunctions to concentrate on the projection of such level sets to the configuration space. We show that at least for a sequence of density $\frac{1}{3}$ of the wavefunctions this property holds and doesn't vanish at high energies. In the correspondent smooth system the potential, $V =$

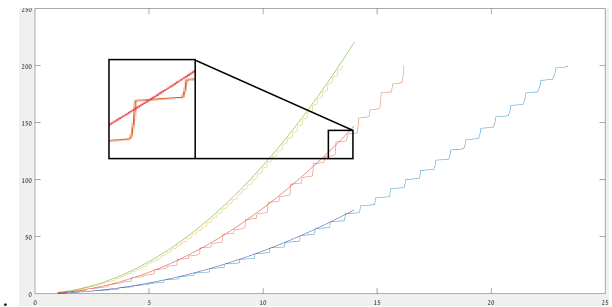


FIG. 3: Weyl's law. Smooth curves correspond to the predicted phase space volume (Eq.10) for the three resonant cases ($\omega_1 = 1, \omega_2 = 1, 2, 3$ yellow, red, blue lines respectively). These prediction fit the corresponding numerical results. The inset shows the non-uniform jump in N for the even m case.

$V_1(q_1) + V_2(q_2)$ is separable. Thus, its wavefunctions, Ψ_n^{sm} , can be written as a product of the wavefunctions of H_i : $\{\Psi_n^{sm}\}_{n=1}^\infty = \Psi_{1,k_1}(q_1)\Psi_{2,k_2}(q_2)$ where $\{\Psi_{i,k_i}\}_{k_i=1}^\infty$ are the wavefunctions of the smooth one dimensional Hamiltonian H_i and $E_{n(k_1,k_2)}^{sm} = E_{k_1} + E_{k_2}$. Since V_i are even:

$$\Psi_{i,k_i}(q_i) = \begin{cases} \Psi_{i,k_i}(-q_i) & \text{if } k_i \text{ is even} \\ -\Psi_{i,k_i}(-q_i) & \text{if } k_i \text{ is odd} \end{cases} \quad (11)$$

When both k_1 and k_2 are odd, the series of wavefunctions $\{\Psi_{n_j(k_1,k_2)}^{sm}\}_{n_j=1}^\infty$ vanishes on both axes, hence, the non-smooth Hamiltonian for the case of step at the origin has a subsequence of wavefunctions of the form:

$$\Psi_{n_j(k_1,k_2)}^{S_0}(q_1, q_2) = \begin{cases} \Psi_{n_j(k_1,k_2)}^{sm} = \Psi_{1,k_1}(q_1)\Psi_{2,k_2}(q_2), & (q_1, q_2) \in \mathbb{R}^2/S_0 \\ 0 & (q_1, q_2) \in S_0 \end{cases} \quad (12)$$

These solutions are smooth in the domain (\mathbb{R}^2/S_0) and satisfy Dirichlet boundary conditions on S_0 . Moreover, $\Psi_{n_j(k_1,k_2)}^{S_0}$ concentrates on the projection of classical level sets; as the one-dimensional wavefunctions are well approximated by the WKB approximation [19], they decay exponentially outside of the classical allowed region of motion:

$$\Psi_{i,k_i}(q_i) \approx C_0 \frac{e^{\theta+i\hbar^{-1} \int \sqrt{2(E_{i,k_i}-V_i(q_i))} dq_i}}{\hbar^{-1/2} \sqrt{2(E_{i,k_i}-V_i(q_i))}}. \quad (13)$$

Next we show that the fraction of such odd wavefunctions for the case of a step at the origin is $1/3$. From equation 3 for the smooth case (i.e. $b = 0$) we deduce that wavefunction that are odd in both directions (odd k_1, k_2) constitute one quarter of all wavefunctions:

$$\lim_{E \rightarrow \infty} \frac{\#\{\Psi_{n_j(k_1,k_2)}^{sm} : E_{n_j} = E_{k_1}^1 + E_{k_2}^2 \leq E\}}{\#\{\Psi_n^{sm} : E_n \leq E\}} = \frac{1}{4}. \quad (14)$$

Since the step is at the origin:

$$\text{Vol}(E)^{S_0} = \frac{3}{4} \text{Vol}(E)^{sm} \quad (15)$$

and thus, by Weyl's law

$$\lim_{E \rightarrow \infty} \frac{\#\{\Psi_{n_j}^{S_0} : E_{n_j} \leq E\}}{\#\{\Psi_n^{S_0} : E_n \leq E\}} = \lim_{E \rightarrow \infty} \frac{\#\{\Psi_{\tilde{n}_j}^{sm} : E_{\tilde{n}_j} \leq E\}}{\frac{3}{4} \#\{\Psi_n^{sm} : E_n \leq E\}} = \frac{1}{3}. \quad (16)$$

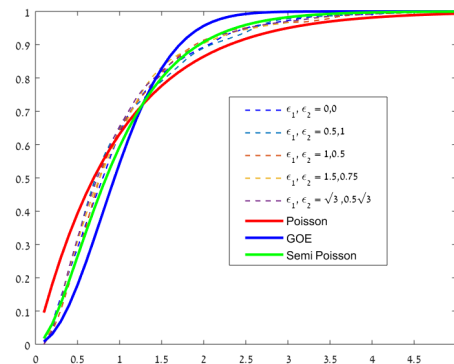
We conclude that for a step at the origin there is no quantum ergodicity in configuration space, and, in fact, there is a positive measure set of eigenfunctions that concentrate on the classical level sets.

To examine the behavior for non-symmetric pseudointegrable cases, we study numerically the shifted corner in the harmonic case: we find the level spacing of the eigenvalues and study the projections to configuration space of the eigenfunctions. Both studies propose that the shift does not break the concentration of a large subset of eigenfunctions on classical level sets.

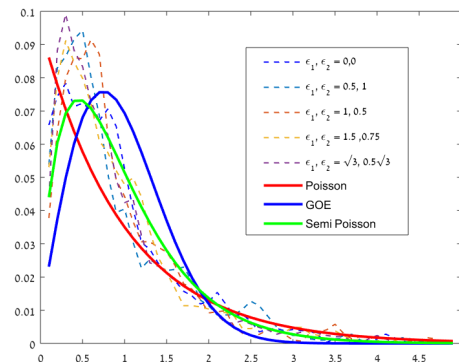
It is convenient for the study of the non-symmetric system to keep the step at the origin and shift the original harmonic potential to have a minimum at $(\epsilon_1, \frac{\epsilon_2}{\omega_2}) = \epsilon \cdot (\cos \alpha, \sin \alpha)$. Then the potential is of the form: $V = U_0 + U_1$ where $U_0 = \frac{q_1^2}{2} + \frac{\omega_2^2 q_2^2}{2}$ and $U_1 = -\epsilon_1 q_1 - \epsilon_2 q_2$. Here, $\epsilon = 0$ corresponds to the system with a step at the origin, and we study the behavior for a non-resonant case at finite values of ϵ , beyond the small perturbation regime. Figure 4a compares the cumulative mean level spacing distribution of this shifted potential of the first 1500 energy levels to the cumulative Poisson distribution (characterizing integrable systems, $N_p(s) = 1 - e^{-s}$, reflecting their locality in the classical phase space) and to the cumulative random matrix ensembles distribution, GOE (characterizing chaotic systems, $N_W(s) = 1 - e^{-\frac{\pi s^2}{4}}$, reflecting their non-local nature in the classical phase space). We obtain intermediate statistics as in pseudo integrable billiards, close to semi-Poisson distribution ($N_{sp}(s) = 1 - e^{-2s}(2s + 1)$) [8] (such a behaviour was also observed in a certain range of parameters in step-like time dependent one d.o.f. Hamiltonian [21]).

Figure 4a shows that the dependence of the level spacing on ϵ appears to be mild and similar to the case $\epsilon = 0$. Recall that in the case of a step at the origin, we showed that there is a positive density sequence of eigenfunctions concentrated on classical level sets. Namely, the level spacing distribution at $\epsilon = 0$ reflects this locality in phase space, together with the non-locality associated with pseudointegrability. Fig. 4a suggests that this behaviour persists when the step is shifted from the origin. In fact, Fig. 4b shows that the distribution with the largest repulsion is achieved at $\epsilon = 0$.

To substantiate the claim that, as suggested by the level spacing plots, at large energies, the general step system still has a positive fraction of wavefunctions that



(a)



(b)

FIG. 4: PDF and CDF of the level spacing for a non-resonant Hamiltonian for several positions of the step. The semi-Poisson distribution (solid thick green line) provides the best fit for all positions of the step (dashed lines), including a step at the origin (blue dashed line). (a) Cumulative distribution functions of Poisson, semi-poisson GOE and numerically calculated CDFs (b) Probability density functions of Poisson, semi-poisson GOE and numerically calculated PDFs. The level spacing are found by a finite differences scheme for the time independent Schrodinger Eq. for the Hamiltonian 1 with $V = U_0 + U_1$ where $U_0 = \frac{q_1^2}{2} + \frac{\omega_2^2 q_2^2}{2}$ and $U_1 = -\epsilon_1 q_1 - \epsilon_2 q_2$. The step is located at the origin and is numerically represented as $V = 10^{28}$. Here, $\omega_1 = 1, \omega_2 = \sqrt{2}$ and $(\epsilon_1, \epsilon_2) = (0, 0), (0.5, 0.25), (1, 0.5), (1.5, 0.75), (\sqrt{3}, \frac{\sqrt{3}}{2})$.

concentrate on classical level sets, we calculate the wavefunctions for such systems. Since the wavefunctions depend continuously on ϵ , for any given maximal energy, for small enough ϵ , such a fraction of concentrated wavefunctions exists. Hence, we first find the natural scaling of ϵ with E and establish that our wavefunction calculations are far from the trivial limit of $\epsilon \rightarrow 0$, namely, that the perturbed wavefunctions do not correlate well with unperturbed wavefunctions.

Expanding the wavefunctions in ϵ , the first order correction to $|n(\epsilon)\rangle = |n^{(0)}\rangle + \epsilon|n^{(1)}\rangle + O(\epsilon^2)$, is:

$$\epsilon|n^{(1)}\rangle = \sum_{k \neq n} \frac{\langle k^{(0)}|U_1|n^{(0)}\rangle}{E_n^{(0)} - E_k^{(0)}} |k^{(0)}\rangle$$

where $U_1 = -\epsilon_1 q_1 - \epsilon_2 q_2$. So for large energies, the number and power of terms that contribute significantly to the sum are expected to stabilize provided we use the scaling: $\epsilon_1 \propto \frac{E_{n+1} - E_n}{q_1}$ and $\epsilon_2 \propto \frac{E_{n+1} - E_n}{q_2}$. Since, for harmonic oscillators, $q_i \propto \sqrt{E}$ and $N(E) \propto \text{Vol}(E) \propto E^2$, so $E_{n+1} - E_n \propto \frac{1}{E}$, we conclude that the stabilization is achieved provided $\epsilon \propto \frac{1}{E^{1.5}}$. As higher orders of the perturbation series give the same result, we actually expect that $|n(\epsilon)\rangle - |n^{(0)}\rangle = O(\epsilon E_n^{1.5})$. To capture the distance between eigenfunctions of the non-perturbed Hamiltonian to the perturbed one around an energy level E_N , we calculate P , the mean squared maximal projection on unperturbed wavefunctions, and T , the mean number of above-threshold contributing unperturbed wavefunctions:

$$P(\epsilon, N; \Delta N, J) = \frac{1}{\Delta N} \sum_{n=N}^{N+\Delta N} \max_{j^0 \leq J} |\langle j^0 | n(\epsilon) \rangle|^2 \quad (17)$$

$$T(\epsilon, N; \Delta N, J, \delta) = \frac{\sum_{n=N}^{N+\Delta N} \#(|\langle j^0 | n(\epsilon) \rangle|^2 > \delta)}{\sum_{n=N}^{N+\Delta N} \sum_{j^0=0}^J \langle j^0 | n(\epsilon) \rangle^2}$$

Figure 5 shows that $P(\epsilon E_N^{3/2}, N; \Delta N, J)$ and $T(\epsilon E_N^{3/2}, N; \Delta N, J, \delta)$ are, to a good approximation, independent of N , supporting the validity of our scaling. Moreover, while for small $\epsilon(\frac{E_N}{E_{301}})^{3/2}$ we see that, as expected, there is a strong correlation between the perturbed and unperturbed wavefunctions, for $\epsilon E_N^{3/2} \geq E_{301}^{3/2}$ the maximal projection, P , is small while the level of mixing, T , is large, indicating that for such values of $\epsilon E^{3/2}$ we are indeed far from the small ϵ limit. Additional computations show that a further increase in $\epsilon E_N^{3/2}$ leads to further decrease in P .

Finally, we show that even when $\epsilon(\frac{E_n}{E_{301}})^{3/2} \gg 1$, i.e. when the wavefunctions are not well approximated by the unperturbed wavefunctions, a substantial fraction of the wavefunctions concentrate on classical level sets. Figure 6 shows the 1481-1500 wavefunctions in Logarithmic scale normalized by the maximal absolute value of the wavefunctions for the unperturbed (step at the origin) and perturbed ($\epsilon = (1.5, 0.75)$) wavefunctions (so $\epsilon(\frac{E_{1500}}{E_{301}})^{3/2} = 5.25$). For both the perturbed and unperturbed systems, wavefunctions that are concentrated along the classical level sets, i.e., are essentially restricted to the configuration space region $(q_1, q_2) \in [q_1^{\min}(E_1, \epsilon_1), q_1^{\max}(E_1, \epsilon_1)] \times [q_2^{\min}(E_2, \epsilon_2, \omega_2), q_2^{\max}(E_2, \epsilon_2, \omega_2)] \setminus S_{q_{wall}}$ where $q_i^{\max, \min}$ correspond to the classical level set boundaries, are clearly seen (e.g. see wavefunction 1 in the unperturbed system and wavefunction 19 in the perturbed system). We call such wavefunctions concentrated wavefunctions.

To quantify this observation, we need to distinguish

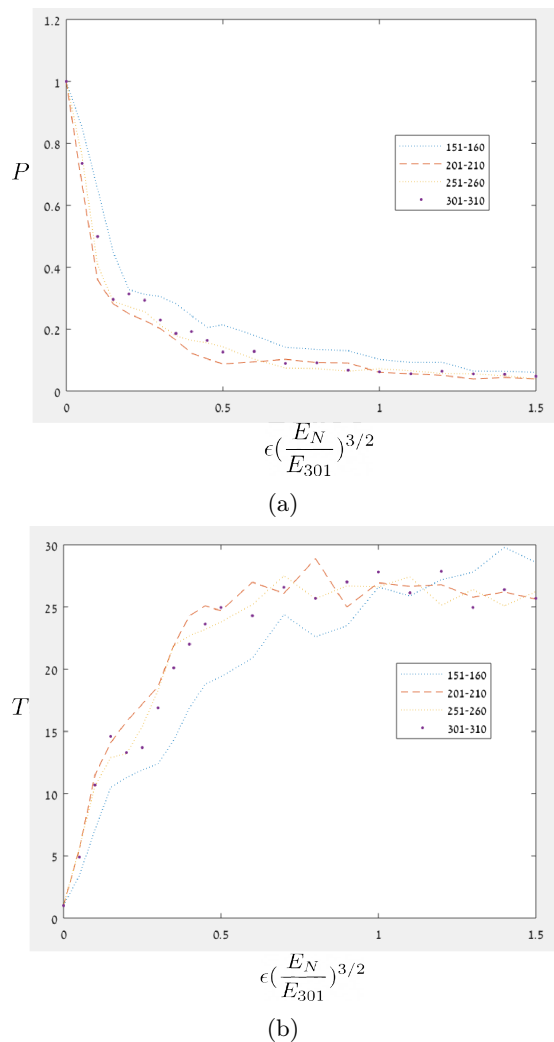


FIG. 5: Scaling of the perturbed wavefunctions with ϵ and energy. (a) The mean squared maximal projection on unperturbed wavefunctions along the energy-scaled ϵ , $\epsilon(\frac{E_N}{E_{301}})^{3/2}$: $P(\epsilon(\frac{E_N}{E_{301}})^{3/2}, N; 10, 400)$ (b) The mean number of above-threshold contributing unperturbed wavefunctions along the energy-scaled ϵ , $\epsilon(\frac{E_N}{E_{301}})^{3/2}$: $T(\epsilon(\frac{E_N}{E_{301}})^{3/2}, N; 10, 400, 0.01)$. These functions are plotted for $N = 151, 201, 251, 301$ for and for several $\epsilon = (\epsilon_1, \epsilon_2 = \frac{\epsilon_1}{2})$ values.

between concentrated wavefunctions from wavefunctions which are not concentrated. To this aim we define vertical and horizontal means of the wavefunctions:

$$M_n^H(q_2) = \int_{-\infty}^{\infty} |\Psi_n(q_1, q_2)|^2 dq_1 \quad (18)$$

$$M_n^V(q_1) = \int_{-\infty}^{\infty} |\Psi_n(q_1, q_2)|^2 dq_2.$$

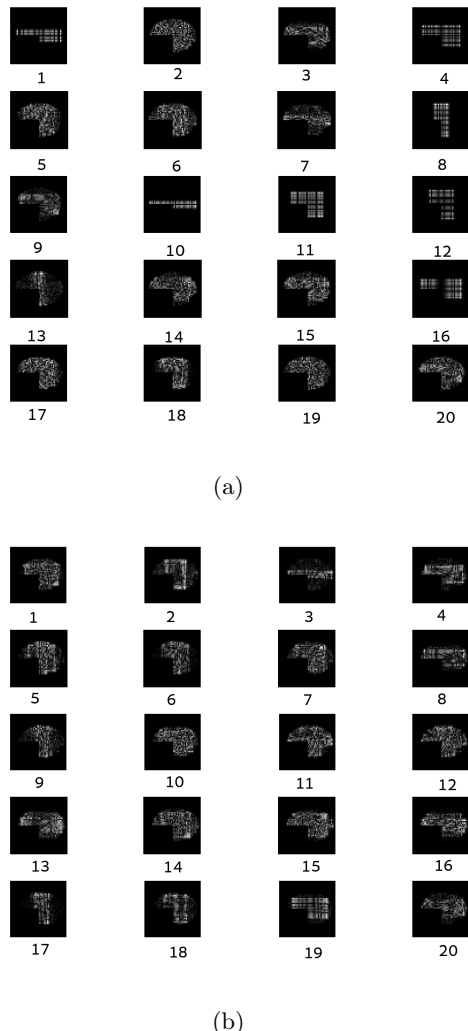


FIG. 6: High energy wavefunctions for a step at the origin and for a shifted step. (a) The unperturbed Hamiltonian. (b) The perturb Hamiltonian with $(\epsilon_1, \epsilon_2) = (1.5, 0.75)$. The wavefunctions for $n = 1481 - 1500$ are plotted. To better visualize the main mass concentration we plot $\text{Log}(|\Psi_n(q_1, q_2; \epsilon)| + \max_{q_1, q_2} |\Psi_n((q_1, q_2; \epsilon))|)$.

and suggest that

$$\tilde{E} = \frac{V_1(\arg \max_{q_1} M_n^V(q_1)) + V_2(\arg \max_{q_2} M_n^H(q_2))}{E} \quad (19)$$

provides a good indicator for the wavefunctions concentration: it is close to one for concentrated wavefunctions and has a much lower value for the rest of the wavefunctions.

Figures 7(a,b) present \tilde{E} values in the case of corner at the origin for low (a) and high (b) ranges of energies. Red points represent \tilde{E} values for the product wavefunctions of Eq. (12) and constitute around 1/3 of the 20 \tilde{E} values. We see that some of the blue points align

with the red ones, while others, around 1/5 for the lower energies and 1/2 for the higher energies have a much lower value. The insets present (M_n^H, M_n^V) in the positive quadrant for the three different types of wavefunctions: for a product wavefunction (red types, wavefunction 1 in 7(a)), for a concentrated wavefunction with a similar \tilde{E} value (blue point, wavefunction 13 in 7(a)) and for a non-concentrated wavefunction with a low \tilde{E} value (blue point, wavefunction 9 in 7(a)). In the first two cases we recognize an oscillatory structure within the classically allowed region, and we observe that the maximal power appears close to the edge. In contrast, the insets corresponding to the low \tilde{E} value show a non oscillatory structure with peaks at arbitrary positions within the Hill region.

Figures 7(c,d) present a similar computation for the case of the shifted potential, $\epsilon = (1.5, 0.75)$, for which there are no product wavefunctions, yet concentrated and not concentrated wavefunction do appear, and the indicator \tilde{E} seems to distinguish between these two types of wavefunctions.

The reasoning for this suggestion is as follows; For step at the origin, for the product wavefunctions (eq. 12), $M_n^H(q_2) = |\Psi_{n,2}(q_2)|^2$ for $q_2 > 0$ and $M_n^H(q_2) = |\Psi_{n,2}(q_2)|^2/2$ for $q_2 < 0$, so by the WKB approximation (eq.13), and similarly for $M_n^V(q_1)$, we indeed expect $\tilde{E} = 1 - f(E)$ for some function $f(E)$ which tends to zero as E goes to infinity (e.g., Figures 7(a,b) suggest that $f(E_{500}) \approx 0.15$, $E_{500} = 39.9$ and $f(E_{1500}) \approx 0.1$, $E_{1500} = 70.5$). For non-product yet concentrated wavefunctions on some classical configuration space region defined by the partial energies (E_1, E_2) , the argmax of $M^{V,H}$ cannot be larger than the corresponding q_i^{max} . Moreover, as classically, one of the momenta components vanishes at the edges of the classical region, the projection of the Liouville measure to the configuration space there is expected to be larger, hence, by the correspondence principle, we expect maximal densities near the edges. Hence, \tilde{E} provides the approximate ratio between the sum of the potential energies at the classical region corners (belonging to the boundary of the classical Hill region) to the total energy, so we expect it to have a similar \tilde{E} values to the corresponding product wavefunctions. In contrast, for a wavefunction which does not concentrate on a single classical level set we do not expect the maxima in the horizontal and vertical directions to lie necessarily on the boundary of the Hill region (see insets corresponding to the lower \tilde{E} values), thus the sum of the potential energies at such an interior point leads to a lower value of \tilde{E} .

In conclusion, Figures 6 and 7 suggest that the fraction of concentrated wavefunctions does not vanish at high energies even when the step is shifted.

Summarizing, we studied the correspondence of a quantum step-oscillator - a two dimensional quantum oscillator in the presence of a step (a step-like region S in the configuration space at which the potential energy is

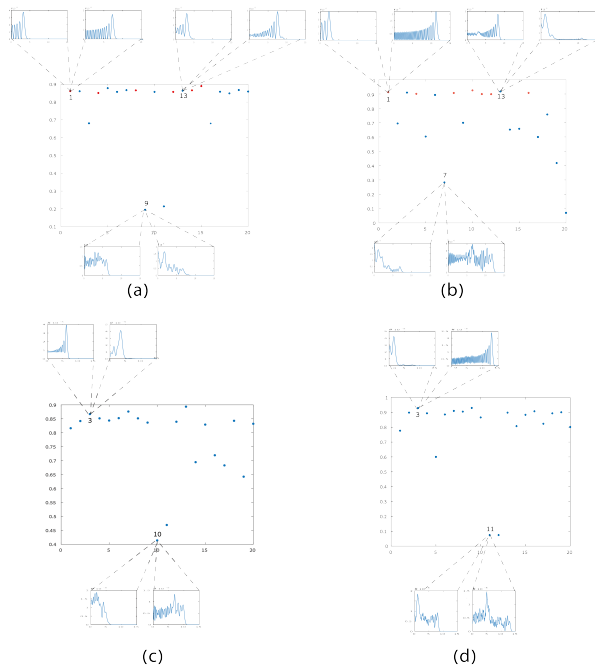


FIG. 7: An indicator for the concentration of wavefunctions on classical level sets. The indicator \tilde{E} of Eq. 19 is plotted for the case of a step at the origin, (a) 481-500 and (b) 1481-1500 wavefunctions (the wavefunctions of Fig. 6a). The indicator \tilde{E} is plotted for the case of a shifted step ($\epsilon = (1.5, 0.75)$) (c) 481-500 and (d) 1481-1500 wavefunctions (the wavefunctions of Fig. 6b). The insets present M^H, M^V for specific points

infinite) to its classical analog, a pseudointegrable Hamiltonian impact system. For the case of harmonic resonant oscillators with a corner at the origin, for which families of periodic orbits can be explicitly constructed, we demonstrated that the EBK quantization condition provides a good predictor to the energy levels (Figure 2), and that Weyl's law provides a good approximation to the growth in the number of wavefunctions (Figure 3). Moreover, we observed that in even-resonance cases two different families of periodic orbits belonging to the same component of the level set co-exist, with distinct corresponding wavefunctions, each contributing a positive portion to the phase space volume (Figure 3). This

demonstrates that the non-ergodicity of level sets has a quantum analog. We showed that the intermediate level spacing of the quantum step-oscillator for non-resonant and not necessarily harmonic potential hardly depends on the position of the step (taken in the negative quadrant) and is approximately semi-Poisson, indicating repulsion of energy levels, similar to the level spacing obtained for pseudointegrable billiards (Figure 4). When the step is at the origin, we showed that there is a positive fraction of wavefunctions that remain concentrated along the classical level sets at arbitrarily high energies, as occurs for integrable systems, namely they do not tend to equidistribute in the configuration space as is the case for pseudointegrable billiards (Eq. (12)-(16) and Figures 6a and 7a,b). Finally, when the corner is shifted from the origin, we conjecture, based on numerical evidence for non-resonant harmonic oscillators, that there is a positive density series of wavefunctions which are not equidistributed and concentrated along the classical level sets (Figures 6b and 7c,d).

Classical Hamiltonian systems with impacts model systems in which strong short range repulsions (such as atomic forces) are combined with attracting forces (such as Van der Waals forces) [22]. Such systems are integrable when the repulsion and attracting forces have sufficiently many common symmetries, and can become pseudointegrable when such symmetries occur along surfaces with corners [17, 23]. Here we propose that the correspondence between such quantum systems and their classical analogs can be studied using both integrable quantization methods (EBK and WKB) and methods used in the study of pseudointegrable billiards (level spacing). The implications of these observations on quantum system that arise in applications, and, in particular, the asymptotic dependence on parameters governing the impact surface geometry (i.e. the singular limit by which corners become smooth), the Ehrenfest time and the evolution of wave packets for such systems is challenging and is left for future studies. The quantum step-oscillators system provides a rich yet simple toy model for studying such questions.

Acknowledgments: VRK is the Estrin family chair of computer science and applied mathematics. We thank the support of ISF grant 787/22. We also thank M. Aizenman, D. Mangoubi, and U. Smilansky for stimulating discussions.

[1] M. V. Berry and M. Tabor, Level clustering in the regular spectrum, *Proceedings of the Royal Society of London. A. Mathematical and Physical Sciences* **356**, 375 (1977).
 [2] O. Bohigas, M.-J. Giannoni, and C. Schmit, Characterization of chaotic quantum spectra and universality of level fluctuation laws, *Physical review letters* **52**, 1 (1984).
 [3] M. V. Berry and M. Robnik, Semiclassical level spacings when regular and chaotic orbits coexist, *Journal of*

Physics A: Mathematical and General **17**, 2413 (1984).
 [4] T. Prosen and M. Robnik, Numerical demonstration of the berry-robnik level spacing distribution, *Journal of Physics A: Mathematical and General* **27**, L459 (1994).
 [5] A. Bäcker, R. Ketzmerick, and A. G. Monastera, Flooding of chaotic eigenstates into regular phase space islands, *Physical review letters* **94**, 054102 (2005).
 [6] P. Richens and M. Berry, Pseudointegrable systems in classical and quantum mechanics, *Physica D: Nonlinear*

- Phenomena **2**, 495 (1981).
- [7] E. Gutkin and C. Judge, The geometry and arithmetic of translation surfaces with applications to polygonal billiards, *Mathematical Research Letters* **3**, 391 (1996).
- [8] E. Bogomolny, U. Gerland, and C. Schmit, Models of intermediate spectral statistics, *Physical Review E* **59**, R1315 (1999).
- [9] S. Zelditch and M. Zworski, Ergodicity of eigenfunctions for ergodic billiards, *Communications in mathematical physics* **175**, 673 (1996).
- [10] E. J. Heller, Bound-state eigenfunctions of classically chaotic hamiltonian systems: scars of periodic orbits, *Physical Review Letters* **53**, 1515 (1984).
- [11] A. Hassell and L. Hillairet, Ergodic billiards that are not quantum unique ergodic, *Annals of Mathematics* , 605 (2010).
- [12] P. Cvitanovic, R. Artuso, R. Mainieri, G. Tanner, G. Vattay, N. Whelan, and A. Wirzba, *Chaos: classical and quantum*, ChaosBook.org (Niels Bohr Institute, Copenhagen 2005) **69**, 25 (2005).
- [13] J. Marklof and Z. Rudnick, Almost all eigenfunctions of a rational polygon are uniformly distributed, *Journal of Spectral Theory* **2**, 107 (2012).
- [14] E. Bogomolny and C. Schmit, Structure of wave functions of pseudointegrable billiards, *Physical review letters* **92**, 244102 (2004).
- [15] A. Kudrolli and S. Sridhar, Experiments on quantum chaos using microwave cavities: Results for the pseudo-integrable l-billiard, *Pramana* **48**, 459 (1997).
- [16] E. Bogomolny, B. Dietz, T. Friedrich, M. Miski-Oglu, A. Richter, F. Schäfer, and C. Schmit, First experimental observation of superscars in a pseudointegrable barrier billiard, *Physical review letters* **97**, 254102 (2006).
- [17] L. Becker, S. Elliott, B. Firester, S. Gonen Cohen, M. Pnueli, and V. Rom-Kedar, Impact hamiltonian systems and polygonal billiards, arXiv preprint arXiv:2001.03726 (2020).
- [18] K. Frączek and V. Rom-Kedar, Non-uniform ergodic properties of hamiltonian flows with impacts, *Ergodic Theory and Dynamical Systems* , 1 (2021).
- [19] M. Brack and R. Bhaduri, *Semiclassical physics* (CRC Press, 2018).
- [20] J. B. Keller, Corrected bohr-sommerfeld quantum conditions for nonseparable systems, *Annals of Physics* **4**, 180 (1958).
- [21] A. M. García-García and J. Wang, Semi-poisson statistics in quantum chaos, *Physical Review E* **73**, 036210 (2006).
- [22] L. Lerman and V. Rom-Kedar, A saddle in a corner—a model of collinear triatomic chemical reactions, *SIAM Journal on Applied Dynamical Systems* **11**, 416 (2012).
- [23] M. Pnueli and V. Rom-Kedar, On the structure of hamiltonian impact systems, *Nonlinearity* **34**, 2611 (2021).
- [24] M. V. Berry and M. Tabor, Closed orbits and the regular bound spectrum, *Proceedings of the Royal Society of London. A. Mathematical and Physical Sciences* **349**, 101 (1976).
- [25] Y. Shimizu and A. Shudo, Polygonal billiards: correspondence between classical trajectories and quantum eigenstates, *Chaos, Solitons & Fractals* **5**, 1337 (1995).